Characterization and physical property studies of Sn, Al doped and co-doped CdO thin films

W. Azzaoui [a,*], M. Medles[a], K. Salim[a], A. Nakrela[a], A. Bouzidi[a], R. Miloua[a,b], M. N. Amroun[a], and M. Khadraoui[a]

[a] *Laboratoire d'Elaboration et de Caractérisation des Matériaux, Département d'Electronique, Université Djillali Liabes, BP89, Sidi Bel Abbés 22000, Algeria.*

[*] *e-mail: walid.azzaoui22@gmail.com; walid.azzaoui@univ-sba.dz*

[b] *Faculté des Sciences de la Nature et de la Vie, Université Ibn Khaldoun 14000 Tiaret, Algeria.*

Received 03 February 2022; accepted 07 June 2022

TM (TM = Sn, AI) doped and co-doped CdO thin films were deposited by spray pyrolysis technique on glass substrate at temperature 350°C. The effect of TM doping and co-doping on the structural, morphological, optical, and electrical properties of CdO thin films was investigated. The obtained films are crystallized in the cubic structure and oriented along the preferential (111) crystallographic plane. The average optical transmittance reaches 79% in the visible range for Sn doped CdO films and 74% for Al-Sn co-doped films. The gap values of the obtained samples are between 2.29 and 2.49 eV. All the deposited films exhibit n-type conductivity with a low electrical resistivity of 7.85×10^{-4} $\Omega.\mathrm{cm}$ obtained for Al doped CdO films.

Keywords: CdO; thin films; co-doped; spray pyrolysis technique.

DOI: https://doi.org/10.31349/RevMexFis.69.011002

1. Introduction

Transparent conductive oxides (TCOs), one of the best choices as the material used in optoelectronic devices such as flat panel displays, photovoltaic cells, smart windows, surface acoustic wave devices, light-emitting diodes, and optical waveguides [1,3], has many TCOs such as Tin oxide $(\mathrm{SnO_2})$ [2], zinc oxide (ZnO) [4], cadmium oxide (CdO) [5]. CdO (cadmium oxide) thin films have sparked substantial attention in recent years because of their numerous advantages such as growth conditions, shape, size, direct and wide bandgap. surface thickness control, low resistivity, and chemical stability [6]. CdO is a group II-VI transparent conductor with a direct bandgap of $2.3-2.7\mathrm{eV}$ and an n-type conductivity with crystallites that are simple cubic crystal systems with an Fm-3m space group and a lattice constant of $4.67\mathring{A}$ [7]. Furthermore, a relatively low electrical resistivity of 10^{-3} to $10^{-4}\Omega\mathrm{cm}$ was used in many optoelectronic applications such as transparent conducting oxides, solar cells, smart windows, optical communications, flat-panel displays, phototransistors, and other types of applications such as IR heat mirrors, gas sensors [8,9,10].

Many processes may be used to obtain un-doped, doped CdO thin films including pulsed laser deposition [11], thermal evaporation[12], sputtering [13], sol-gel [14], Metallo-organic chemical vapor deposition (MOCVD) [15], electrospinning[16], and spray pyrolysis [17]. Among these approaches, spray pyrolysis remains appealing and interesting due to its low cost, simplicity, speed, and ability to create large-area coatings.

It has been shown, according to the literature, that the physical properties of CdO thin films can be improved by introducing an appropriate dopant with a covalent radius less than or to that of the host lattice atoms. On the on the other hand, it could be interesting to explore the incorporation of two types of dopant elements instead of one to examine their effects on the CdO films properties.

In the present work, the prepared $\mathrm{TM}(\mathrm{TM} = 3\%\mathrm{Sn}, 1\%\mathrm{Al})$ doping and $1\mathrm{at}\%\mathrm{Al} + 3$ at $\%$ Sn co-doping of CdO thin films by spray pyrolysis method have been investigated.

2. Experimental details

The Transition Metal $(\mathrm{TM} = \mathrm{Sn}, \mathrm{Al})$ doped and $\mathrm{Al}-\mathrm{Sn}$ co-doped CdO thin films were deposited from a $0.1\mathrm{M}$ on soda-lime glass substrates with 1% Al doping, $3\%\mathrm{Sn}$ doping and combined 1% Al with 3% Sn as co-doping by spray pyrolysis technique (Fig. 1). The starting chemical solutions were prepared by dissolving cadmium acetate $(\mathrm{Cd}\,(\mathrm{CH_3(COO)_2 2H_2O})$ in double distilled water, Aluminum nitrate $(\mathrm{Al}\,(\mathrm{NO_3})\,9\mathrm{H_2O})$ and tin chloride $(\mathrm{Sn}\,(\mathrm{Cl_2})\,2\mathrm{H_2O})$. Furthermore, all the obtained films were manufactured under the same conditions summarized in

TABLE I. Deposition conditions of the obtained thin films.

Chemical precursors	Cadmium acetate (Cd $(CH_3(COO)_2.2H_2O)$
Deposit temperature	$350 \pm 10°\mathrm{C}$
Distance between atomizer and hotplate	27 cm
Spray solution flow rate	1 ml/min
volume of sprayed solution	10 ml

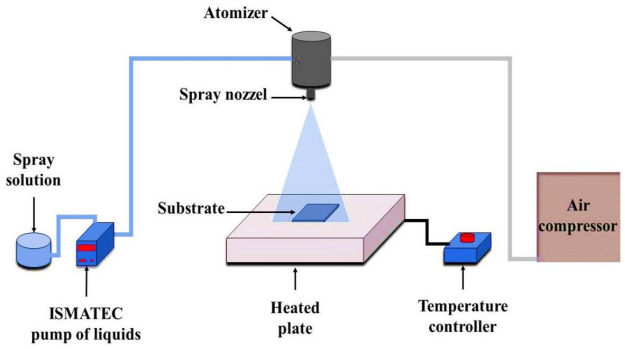

FIGURE 1. Spray pyrolysis Scheme.

TABLE II. Samples designations.

Designations	Samples
CdO Undoped	CdO
CdO doped 1% Al	ACO
CdO doped 3% Sn	TCO
CdO co-doped 1% Al 3% Sn	ATCO

Table I. The sample designations listed in Table II will be utilized in the discussing part. To remove and clean surface contaminants, the substrates were cleaned in an ultrasonic bath with ethanol for 5 minutes before being washed with double distilled water. Following the growth procedure, the coated substrates were allowed to cool naturally to ambient temperature.

3. Results and discussion

3.1. Structural properties

The structural characterization was performed at room temperature using a Bruker X-ray diffractometer model $D2$ Phaser with CuKα radiation $\lambda = 1.5406$ Å.

Figure 2 shows the XRD patterns of the deposited thin films. It reveals that the diffracted peaks located at $2\theta = 33.02°$, $38.38°$, $55.36°$, $65.90°$ and $69.26°$ are linked to the plans of the miller (111), (200), (220), (311) and (222) respectively, which are in good agreement with JCPD Card No; 05-0640. All prepared samples have a cubic structure with an orientation plane (111). Similar results were reported in the literature [18]. No crystalline phases of Al or Sn one neither their oxides were observed, which suggests the incorporation success of Al^{3+} and Sn^{4+} ions into the CdO lattice [19].

From Fig. 2, we notice that the intensity of peak (111) increases slightly after doping, which could be attributed to the dopant incorporations into the CdO matrix of our obtained films. This behavior has been, already, observed in literature [8,20]. The average crystallites size of the films was calculated using the Scherrer formula [21].

$$D = \frac{0.9\lambda}{\beta \cos\theta}, \tag{1}$$

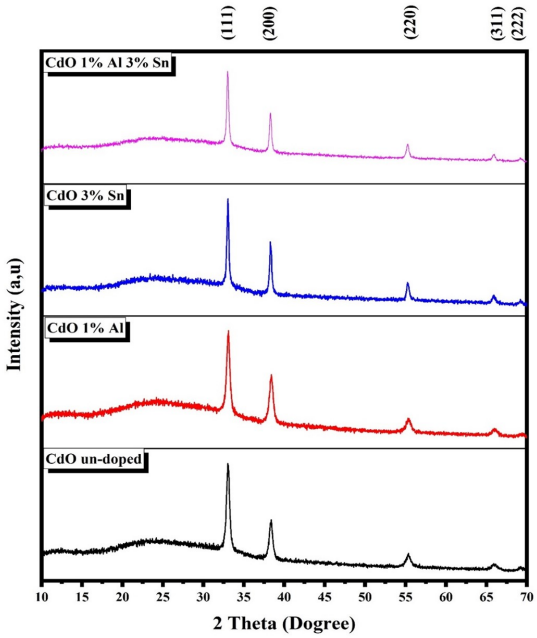

FIGURE 2. XRD patterns of CdO, ACO, TCO and ATCO thin films.

where D is the crystallite size, λ(1.5406 Å), β is the FWHM (Full Width Half Maximum) in radians of the peak (111) and θ is the Braggs angle. From the Table III, it is seen that the crystallite size increased with Sn doped and Al-Sn co-doping.

The constant lattice a, strain ε, and dislocation density δ for CdO films determined using the following relationships [22,23].

$$d = \frac{a}{\sqrt{(h^2 + l^2 + k^2)}}, \tag{2}$$

$$\varepsilon = \frac{\beta \cos\theta}{4}, \tag{3}$$

$$\delta = \frac{1}{D^2}. \tag{4}$$

As shown in Table III, the crystallite size of the CdO films decreased with 1% Al doping. This decrease could be attributed to the strained crystal growth due the Al incorporation [24]. On the other hand, the crystallite size TCO and ATCO thin films increased with tin and aluminium incorporation which explains the improvement of the crystallinity of the films. The value of the lattice parameter of the CdO obtained films decreases with Al and Sn doping and increases with the Al-Sn co-doping. This change tendency of the lattice parameter value with doping and co-doping could be explained the substitution of Cd^{2+} ions with Al^{3+} and Sn^{4+} ones in CdO matrix as well as the Al and Sn atom migrating in the grain boundaries [25].

3.2. Optical properties

The optical transmittances were recorded using a JASCO 570 type UVvisible-NIR double-beam spectrophotometer.

TABLE III. Structural parameters of CdO, ACO, TCO and ATCO thin films.

Samples	$(2\theta)^\circ$ (111)	a(Å) D(nm)	Crystallite size	Strain $\cdot 10^{-3}$	FWHM $\cdot 10^{-3}(^\circ)$	Density dislocation $\cdot 10^{-3}$ (Line/nm^2)
CdO	33.02	4.6948	17.27	2.00	8.37	3.35
ACO	33.10	4.6838	16.21	2.13	8.92	3.80
TCO	33.04	4.6921	29.04	1.19	4.98	1.18
ATCO	33.00	4.6976	29.69	1.16	4.87	1.13

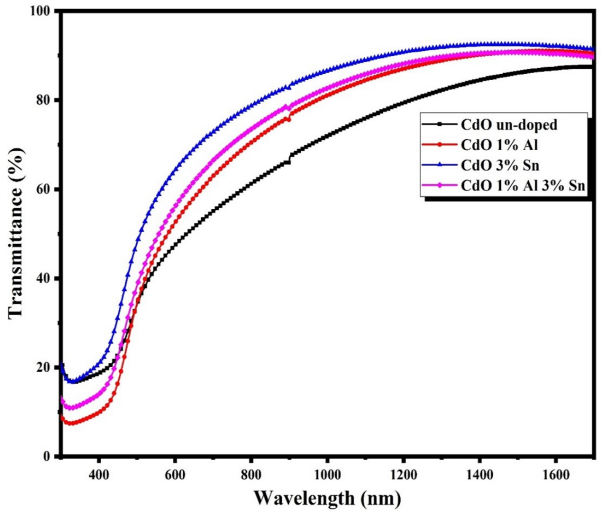

FIGURE 3. Optical transmittance spectra of CdO, ACO, TCO and ATCO thin films.

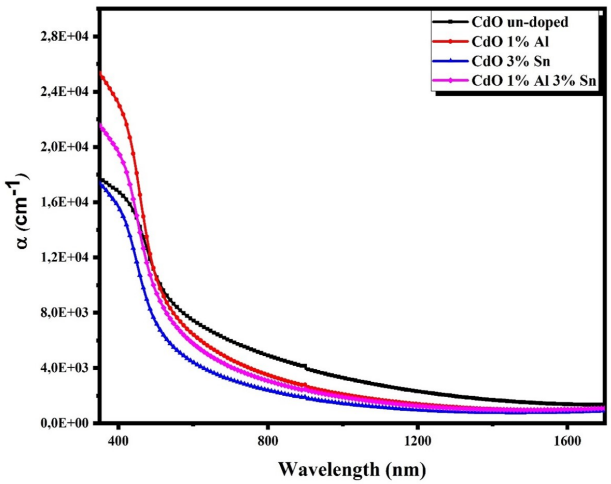

FIGURE 4. Absorption coefficient spectra of CdO, ACO, TCO and ATCO thin films.

Figure 3 shows the optical transmittances in the wavelength range of 300-1700 nm of the prepared thin films. An average transmission of 61-79% has been observed in the visible region. The optical transparency of the films has been clearly increased and reached a maximum value around 79% for TCO thin films. This optical transparency improvement could be explained by the crystallinity enhancement of the TCO films (Table III). It is well known that changes in transmittance values depend on the characteristics of the materials, such as crystalline quality, surface morphology, and free carrier concentrations in films [18].

The variations curves of the absorption coefficient α were estimated using the following relation [18].

$$\alpha = \frac{\ln \frac{1}{T}}{t}, \tag{5}$$

where T is the transmittance and t is the film thickness. The evolutions of the absorption coefficients with wavelength for the obtained thin films are shown in Fig. 4. This figure shows that α values are in the order of 10^{+4} cm^{-1} which is in good agreement with literature [26]. The optical band gaps of the obtained films were determined with Tauc relation [27].

$$(ahv)^n = A(hv - Eg), \tag{6}$$

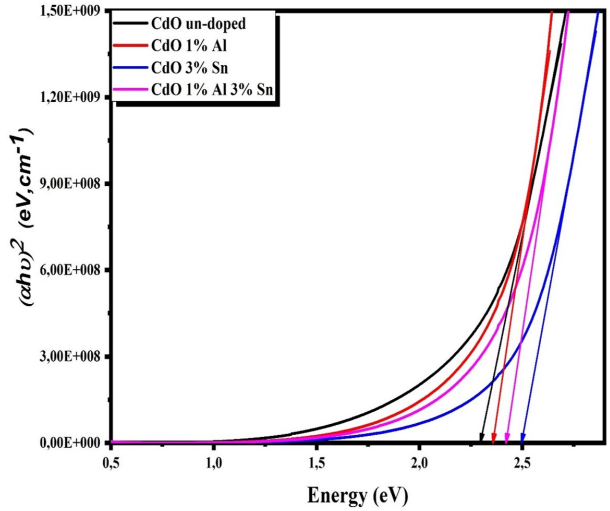

FIGURE 5. $(ahv)^2$ spectra of CdO, ACO, TCO and ATCO thin films.

where α is the absorption coefficient, hv the photon energy, A constant and Eg the optical band gap. We take $n = 2$ for direct band gap semiconductor.

The band gap value of un-doped CdO films is estimated as 2.29 eV which agrees with the literatures [6]. The optical

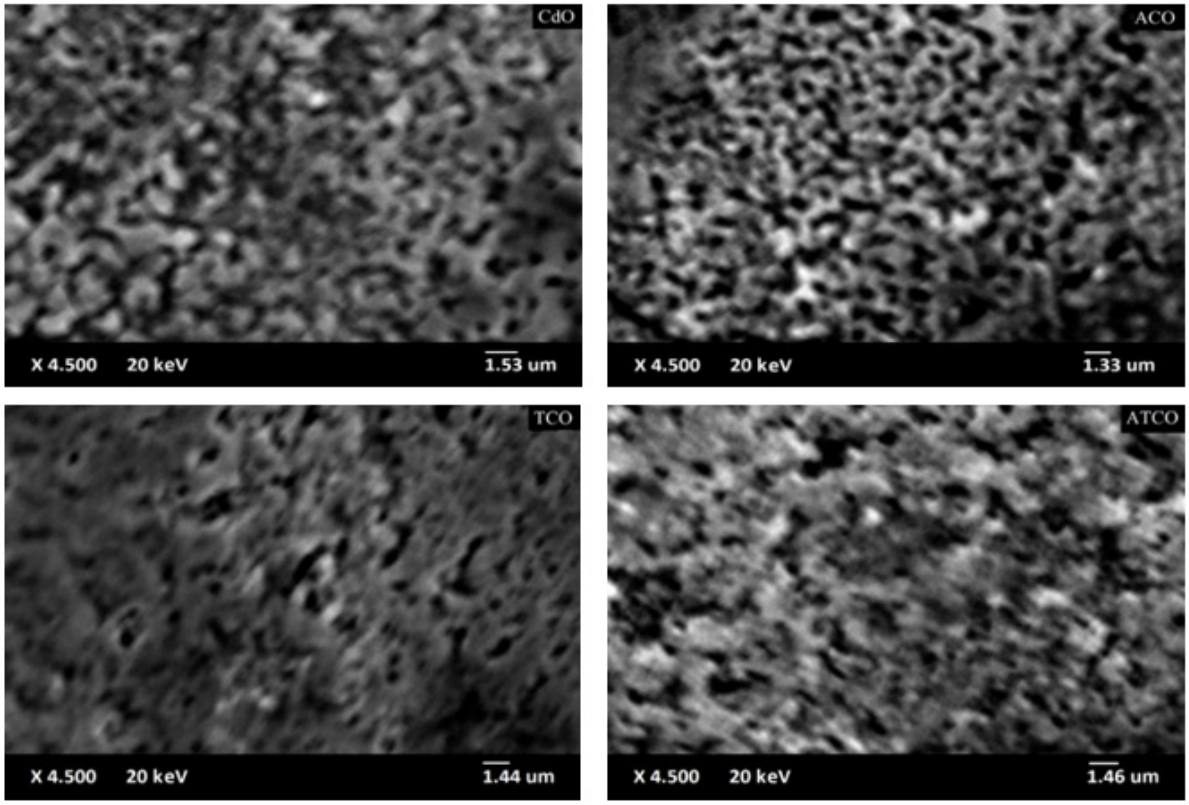

FIGURE 6. SEM images of CdO, ACO, TCO and ATCO thin films.

TABLE IV. Direct band gap and urbach energy of CdO, ACO, TCO and ATCO thin films.

Samples	Direct band gap energy Eg (eV)	Urbach energy (eV)
CdO	2.29	0.78
ACO	2.35	0.61
TCO	2.49	0.57
ATCO	2.42	0.60

gap increased from 2.29 eV for CdO films to 2.49 for TCO (Fig. 5), this increase could be explained by the contribution of the Moss-Burstein effect [28,29].

The Urbach energy Eu was estimated by using the following expression [30]

$$a = a_0 \exp\left(\frac{h\upsilon}{Eu}\right), \tag{7}$$

where a_0 is a constant and Eu the Urbach energy. The values of Eu are determined from the reciprocal of the slope of the relation between In a and $h\upsilon$, and the obtained results are summarized in Table IV. We observe that Eu values change inversely with direct optical band gaps for the co-doped films, confirming the minimization of defect states in the prepared films [31].

TABLE V. Element concentrations in CdO, ACO, TCO and ATCO thin films.

	Concentration at. %				
	Cd	O	Si	Al	Sn
CdO	31.64	38.71	29.65	-	-
ACO	31.34	35.25	31.98	1.43	-
TCO	30.17	35.16	33.07	-	1.60
ATCO	54.06	30.48	10.50	2.06	2.90

3.3. Morphological and EDX

The surface morphology and the chemical composition analyses were carried out using a Jeol JSM 5800 scanning electron microscope which is equipped with an energy dispersive X-ray detector (EDX, IXRF Model 550i). The surface morphologies of the obtained thin films are presented in Fig. 6. This figure indicated that the deposited films are dense and no cracks are observed on large scan area. The chemical composition checking by the EDX spectra, is given in the Fig. 7. EDX spectra shown the presence of Cd, Sn, Al and O in the obtained thin films, the presence of Si (the most intense peak) is due to the substrate effect. The reported EDX data confirms the previous XRD analysis. The chemical compositions in percentage are summarized in Table VI.

TABLE VI. Electrical parameters of CdO, ACO, TCO and ATCO at room temperature.

Samples	Resistivity (Ω.cm)	Mobility ($\mathrm{cm}^2/\mathrm{Vs}$)	Carrier (cm^{-3}) Concentrations	Sheet Resistance (Ω/sq)	Hall Coefficient (cm^3/C)
CdO	$1.85.10^{-3}$	4.83	$6.95.10^{+20}$	185.73	$-8.98.10^{-3}$
ACO	$7.85.10^{-4}$	11.58	$6.85.10^{+20}$	78.56	$-9.25.10^{-3}$
TCO	$3.92.10^{-2}$	0.28	$5.59.10^{+20}$	3920.00	$-1.11.10^{-2}$
ATCO	$6.04.10^{-3}$	1.32	$7.78.10^{+20}$	604.98	$-8.02.10^{-3}$

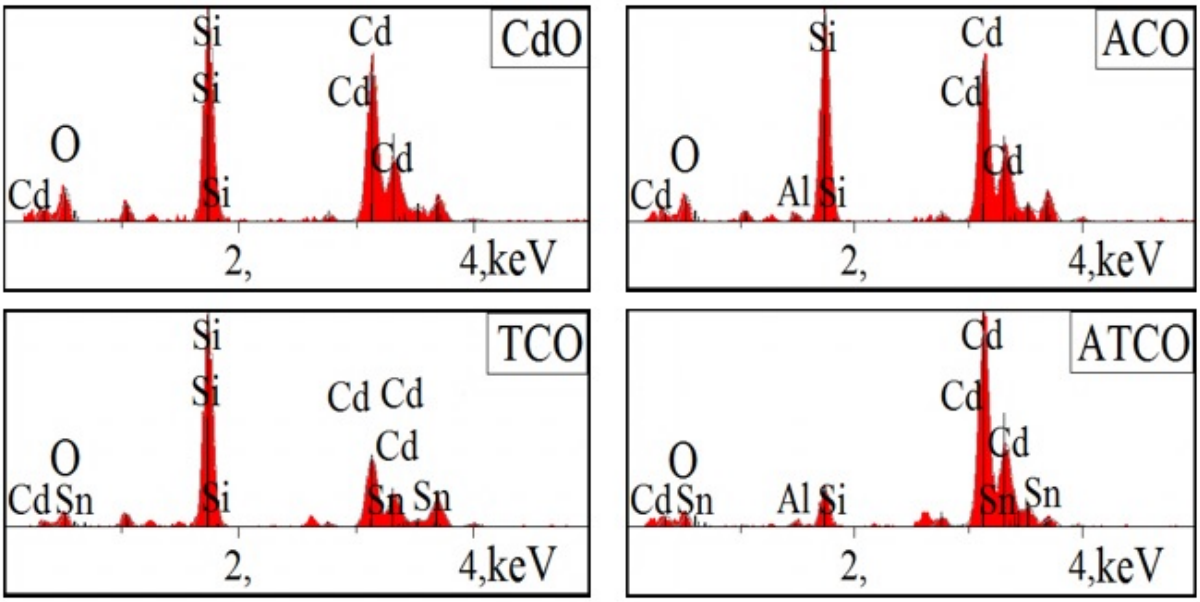

FIGURE 7. Energy dispersive X-ray (EDX) spectra, of CdO, ACO, TCO and ATCO thin films.

3.4. Electrical properties

The electrical properties were performed by ECOPIA HMS-5000 Hall Effect measurement system at room temperature. The carrier concentration n, mobility μ and resistivity ρ of the obtained films are presented in Table VI. The negative sign of the Hall coefficient confirms the n-type conductivity of our films which is in agreement with literatures [32]. The carrier concentrations are in the order of 10^{+20} cm^{-3}. The resistivity of the obtained films decreased from 1.85×10^{-3} Ωcm for un-doped CdO films to 7.85×10^{-4} Ωcm for ACO films which is attributed to the increases in mobility and decrease in sheet resistance. The resistivity decreasing of the CdO films with Al incorporation has been already reported in literature [32].

4. Conclusion

In this work, the XRD results demonstrate that all the films have a cubic structure with an orientation plane (111). The obtained samples are transparent in the visible region with an average of transmittance value which could be increased from 61 % to 79 % with Sn doping. The optical band gap Broadening from 2.29 to 2.49 eV could be attributed to the BursteinMoss effect. The resistivity value minimum was observed for the ACO samples (7.85×10^{-4} Ωcm). The results presented in this study showed that Sn and/or Al incorporation in CdO thin films improve their physical properties films.

Acknowledgments

The authors would like to acknowledge the financial support of this work from the General Direction of Scientific Research and Technology (DGRSDT/MESRS) of Algeria, under PRFU project n° A10N01UN220120200008.

1. L. L. Pan, G. Y. Li, and J. S. Lian. Structural,optical and electrical properties of cerium and gadolinium doped CdO thin films. *Applied surface science* **274** (2013) 365-370, https://doi.org/10.1016/j.apsusc.2013.03.066
2. A. H. Yahi *et al*., The relationship between processing and structural, optical, electrical properties of spray pyrolysed SnO2 thin films prepared for different deposition times. Optik **169** (2019) 163198, https://doi.org/10.1016/j.ijleo.2019.163198
3. G. Murtaza *et al.*, Structural, electronic and optical properties of CaxCd1-xO and its conversion from semimetal to wide bandgap semiconductor. *Computational Materials Science* **58** (2012) 71-76, https://doi.org/10.1016/j.commatsci.2012.01.020
4. A. Nakrela *et al.*, Site location of Al-dopant in ZnO lattice by exploiting the structural and optical characterisation of ZnO: Al thin films. *Results in Physics* **5** (2016) 133-138, https://doi.org/10.1016/j.rinp.2016.01.010.
5. S. C. Colak, *et al*., Characterization of chemically sprayed CdO films on borate and phosphate glass substrates produced by melt-quenching technique. *Materials Chemistry and Physics* **138.1** (2013) 327-332, https://doi.org/10.1016/j.matchemphys.2012.11.064.
6. H. Güney, and D. Iskenderoulu, The effect of Zn doping on CdO thin films grown by SILAR method at room temperature. *Physica B: Condensed Matter* **252** (2019) 119-123,https://doi.org/10.1016/j.physb.2018.09.045.
7. A. A. Dakhel, Bandgap narrowing in CdO doped with europium. *Optical Materials* **31.4** (2009) 691-695, https://doi.org/10.1016/j.optmat.2008.08.001
8. M. Anitha *et al*., Influence of a novel co-doping (Zn+ F) on the physical properties of nano structured (1 1 1) oriented CdO thin films applicable for window layer of solar cell. *Applied surface science* **343** (2018) 55-67, https://doi.org/10.1016/j.apsusc.2018.02.231
9. A. A. Dakhel, Effect of thallium doping on the electrical and optical properties of CdO thin films. *Physica status solidi (a)* **205.11** (2008) 2704-2710, https://doi.org/10.1002/pssa.200723472
10. P. Velusamy *et al*., Highly transparent conducting cerium incorporated CdO thin films deposited by a spray pyrolytic technique. *RSC advances* **5.124** (2015) 102741-102749, https://doi.org/10.1039/c5ra15262c.
11. M. Yan, *et al*., Highly conductive epitaxial CdO thin films prepared by pulsed laser deposition. *Applied Physics Letters* **78.16** (2001) 2342-2344, https://doi.org/10.1063/1.1365410.
12. A. A. Dakhel, and F. Z. Henari, Optical characterization of thermally evaporated thin CdO films. Crystal Research and Technology: *Journal of Experimental and Industrial Crystallography* **38.11** (2003) 979-985, https://doi.org/10.1002/crat.200310124
13. T. K. Subramanyam, S. Uthanna, and B. Srinivasulu Naidu. Preparation and characterization of CdO films deposited by dc magnetron reactive sputtering. *Materials Letters* **35.3-4** (1998) 214-220, https://doi.org/10.1016/S0167-577X(97)00246-2
14. M. Tufiq Jamil *et al.*, Effect of Re and Tm-site on morphology structure and optical band gap of ReTmO 3 (Re= La, Ce Nd, Gd, Dy, Y and Tm= Fe, Cr) prepared by sol-gel method. *Rev. Mex. Fis.* **64.4** (2018) 381-391, https://doi.org/10.31349/RevMexFis.64.381.
15. S. Jin, *et al.*, Dopant ion size and electronic structure effects on transparent conducting oxides. Sc-doped CdO thin films grown by MOCVD. *Journal of the American Chemical Society* **126.42** (2004) 13787-13793, https://doi.org/10.1021/ja0467925.
16. A. M. Bazargan *et al*., Electrospinning preparation and characterization of cadmium oxide nanofibers. *Chemical Engineering Journal* **155.1-2** (2009) 523-527,https://doi.org/10.1016/j.cej.2009.08.004.
17. K. Salim *et al*., Enhancement of optical and electrical properties of spray pyrolysed ZnO thin films obtained from nitrate chemical by Al-Sn co-doping. *Optik* **210** (2020) 164504, https://doi.org/10.1016/j.ijleo.2020.164504.
18. M. Anitha et al., Effect of Zn doping on structural, morphological, optical and electrical properties of nebulized spray-deposited CdO thin films. *Applied Physics A* **124.8** (2018) 1-13, https://doi.org/10.1007/s00339-018-1993-7.
19. K. Usharani, and A. R. Balu. Structural, optical, and electrical properties of Zn-doped CdO thin films fabricated by a simplified spray pyrolysis technique. *Acta Metallurgica Sinica (English Letters)* **28.1** (2015) 64-71, https://doi.org/10.1007/s40195-014-0168-6.
20. N. Manjula *et al*., Enhancement in some physical properties of spray deposited CdO: Mn thin films through Zn doping towards optoelectronic applications. *Optik* **127.16** (2016) 6400-6406, https://doi.org/10.1016/j.ijleo.2016.04.129.
21. K. Salim, M. N Amroun, and W. Azzaoui. Influence of Doping Concentration on the Properties of Tin Doped Zinc Oxide Thin Films Prepared by Spray Pyrolysis for Photovoltaic Applications. *International Journal of Thin Film Science and Technology* **10.3** (2021) 9,http://dx.doi.org/10.18576/ijtfst/100309.
22. H. Güney, The structural, morphological, optical and electrical properties of Pb doped CdO thin films grown by spray method. *Vacuum* **159** (2019) 261-268, https://doi.org/10.1016/j.vacuum.2018.10.053.
23. K. Salim *et al*., Effect of Mn Doped and Mn+ Sn Co-doping on the Properties of ZnO Thin Films. *International Journal of Thin Film Science and Technology* **10.3** (2021) 13, http://dx.doi.org/10.18576/ijtfst/100313.
24. N. Raja, et al., Structural, optical, electrical and catalytic properties of precursor solution-aged spray deposited undoped, Zn-doped and Ag-doped CdO thin films. *Bulletin of Materials Science* **43.1** (2020) 1-12, https://doi.org/10.1007/s12034-020-02088-5.
25. A. Gencer Imer, Investigation of Al doping concentration effect on the structural and optical properties of the nanostructured CdO thin film. *Superlattices and Microstructures* **92** (2016) 278-284, https://doi.org/10.1016/j.spmi.2016.01.035.

26. R. Kumaravel, K. Ramamurthi, and V. Krishnakumar. Effect of indium doping in CdO thin films prepared by spray pyrolysis technique. J*ournal of Physics and Chemistry of Solids* **71.11** (2010) 1545-1549, https://doi.org/10.1016/j.jpcs.2010.07.021.

27. M. N. Amroun, and M. Khadraoui. Effect of substrate temperature on the properties of SnS2 thin films. *Optik* **184** (2019) 16-27, https://doi.org/10.1016/j.ijleo.2019.03.011.

28. E. Burstein, Anomalous optical absorption limit in InSb. *Physical review* **93.3** (1954) 632, https://doi.org/10.1103/PhysRev.93.632.

29. Moss, TS1954. The interpretation of the properties of indium antimonide. *Proceedings of the Physical Society. Section B* **67.10** (1954) 775,https://doi.org/10.1088/0370-1301/67/10/306.

30. M. N. Amroun *et al.*, Investigation on the structural, optical and electrical properties of mixed SnS2-CdS thin films. *Optik* **131** (2017) 152-164, https://doi.org/10.1016/j.ijleo.2016.11.005.

31. K. Usharani, and A. R. Balu, Properties of spray deposited Zn, Mg incorporated CdO thin films. *Journal of Materials Science: Materials in Electronics* **27.2** (2016) 2071-2078,https://doi.org/10.1007/s10854-015-3993-0.

32. R. Kumaravel *et al*., Electrical, optical and structural properties of aluminum doped cadmium oxide thin films prepared by spray pyrolysis technique. *Materials Chemistry and Physics* **122.2-3** (2010) 444-448,https://doi.org/10.1016/j.matchemphys.2010.03.022.